ORIGINAL ARTICLE

Emergence, phylogeography, and adaptive evolution of mpox virus

Haifei Guan[a,b], Ijaz Gul[a,b], Chufan Xiao[a,b], Shuyue Ma[a,b], Yingshan Liang[a], Dongmei Yu[c], Ying Liu[d], Hong Liu[d], Can Yang Zhang[a], Juan Li[e] and Peiwu Qin[a,b]

a *Institute of Biopharmaceutical and Health Engineering, Tsinghua Shenzhen International Graduate School, Tsinghua University, Shenzhen, 518055, China,* b *Tsinghua-Berkeley Shenzhen Institute, Tsinghua Shenzhen International Graduate School, Tsinghua University, Shenzhen, 518055, China,* c *School of Mechanical, Electrical & Information Engineering, Shandong University, Weihai, Shandong, 264209, China,* d *Food Inspection & Quarantine Center, Shenzhen Custom, Shenzhen, Guangdong, 518060, China and* e *Advanced Research Institute for Multidisciplinary Science, Beijing Institute of Technology, Beijing, 100081, China*

Abstract

Mpox (Monkeypox) is a zoonotic disease caused by mpox virus (MPXV). A multi-country MPXV outbreak in non-endemic demographics was identified in May 2022. A systematic evaluation of MPXV evolutionary trajectory and genetic diversity could be a timely addition to the MPXV diagnostics and prophylaxis. Herein, we integrated a systematic evolution analysis including phylogenomic and phylogeographic, followed by an in-depth analysis of the adaptive evolution and amino acid variations in type I interferon binding protein (IFNα/βBP). Mutations in IFNα/βBP protein may impair its binding capacity, affecting the MPXV immune evasion strategy. Based on the equilibrated data, we found an evolutionary rate of 7.75×10^{-5} substitutions/site/year, and an earlier original time (2021.25) of the clade IIb. We further discovered significant genetic variations in MPXV genomes from different regions and obtained six plausible spread trajectories from its intricate viral flow network, implying that North America might have acted as a bridge for the spread of MPXV from Africa to other continents. We identified two amino acids under positive selection in the Rifampicin resistance protein and extracellular enveloped virus (EEV) type-I membrane glycoprotein, indicating a role in adaptive evolution. Our research sheds light on the emergence, dispersal, and adaptive evolution of MPXV, providing theoretical support for mitigating and containing its expansion.

Keywords: Mpox virus, Evolution, Phylogeographic, IFNα/βBP, *Orthopoxvirus*
Original Submission: 6 December 2022; **Revised Submission:** 14 February 2023; **Accepted:** 15 February 2023
Article published online: 18 February 2023

Corresponding author. Institute of Biopharmaceutical and Health Engineering, Tsinghua Shenzhen International Graduate School, Tsinghua University, Shenzhen, 518055, China.
Corresponding author.
E-mail: pwqin@sz.tsinghua.edu.cn

1. Introduction

Mpox (Monkeypox) virus (MPXV) is a double-stranded DNA virus belonging to the genus *Orthopoxvirus* and *Poxviridae* family [1], which includes vaccinia virus (VACV), variola virus (VARV), cowpox virus (CPXV), camelpox virus (CMLV), buffalopox virus (BPXV), and ectromelia virus (ECTV). Mpox is a zoonotic disease manifesting similar clinical symptoms to smallpox [2]. MPXV was first identified in monkeys in 1958 [3], then reported in humans in the Democratic Republic of the Congo (DRC) in 1970 [4], and there were constant spillover events to other hosts [5]. Before the current outbreak, MPXV was predominantly circulated in Africa, with only a few sporadic cases in other continents. However, the outbreak of mpox in non-endemic regions has recently garnered substantial research attention.

Differing from previous mpox outbreaks, the current infected cases are not significantly related to travel history from endemic regions or contact with infected animals. From Jan 2022 to Feb 12, 2023, the World Health Organization (WHO) has reported 85,765 confirmed mpox cases and 93 deaths in 110 countries or territories [6]. Mpox has now been declared a

https://doi.org/10.1016/j.nmni.2023.101102

global health emergency [7]. The termination of smallpox vaccination and weakened smallpox immunity in the general population could be attributed to mpox reemergence [8,9]. Overall, the ongoing epidemic is atypical, with a more convoluted transmission pattern and a larger aggregated outbreak, necessitating a comprehensive investigation of the prevailing MPXV epidemiology [10].

MPXV's immune evasion may play a pivotal role in virus spread and mutation. Interferons (IFNs), a family of cytokines that inhibits viral replication, are one of the key effectors of the innate immune response [11,12]. Poxviruses utilize several strategies to counteract the IFNs' protective effects and thus escape the immune response. For instance, the E3L gene product of VACV competitively binds double-stranded RNA and blocks IFN-induced and dsRNA-induced activation of the protein kinase R (PKR) [13]. Another study proposes the likely role of K3L gene product in VACV host immune escape. The inhibition of the phosphorylation of host eukaryotic initiation factor 2α (eIF2α) by competitive binding of K3L gene product to PKR may impart IFN resistance [14]. However, these mechanisms can only block the IFNs response in infected cells, and both E3L ortholog and K3L ortholog are truncated and inactivated in MPXV [15], hence the IFNs evade strategy of MPXV mainly depends on the expression of the soluble type I interferon binding protein (IFNα/βBP). Previous studies have shown that poxviruses shield cells from IFN by binding cells through soluble IFNα/βBPs, permitting poxvirus proliferation and therefore, interfering with host immune function [16,17]. Unlike the type I IFN cellular receptors have fibronection type III domains, the IFNα/βBPs encoded by VACV B18R, MPXV B16R, and other *orthopoxviruses* genes, are glycoproteins with three immunoglobulin (Ig)-like domains [18]. However, the mechanism of MPXV IFNα/βBP remains to be deciphered, and it is questionable whether the variation in IFNα/βBP is one of the reasons for MPXV's lower pathogenicity.

Several studies have conducted phylogenomic analysis of MPXV [19,20], demonstrating that the current outbreak originates from West Africa and attempting to explore the generation time of the most recent common ancestor (tMRCA). However, most of the reported studies simply picked all accessible data and used unfiltered data, which would make the results untrustworthy owing to the large number and high similarity of currently reported sequences [21,22]. Furthermore, phylogeographic methods have been widely used in recent years to elucidate the transmission history of viral epidemics, which is crucial for viral prevention and control, but detailed studies on the phylogeography of MPXV are still lacking.

To fill these gaps, we integrated the phylogenetic analysis with spatiotemporal information to investigate how MPXV populations varied and diffused. Via the phylodynamic approaches, we provided an insight into MPXV evolutionary potential, which may be unique amongst viral evolution processes. Finally, we predicted the role of MPXV immunomodulatory proteins in MPXV pathogenesis.

2. Materials and methods

2.1. Dataset of MPXV genomes and genome alignment

All MPXV sequences with complete genomes were downloaded from GenBank (https://www.ncbi.nlm.nih.gov/, accessed on August 8, 2022), and annotated with time and country as dataset 1. Sequences lacking information about time and country were removed from dataset 1 (Table S1). Dataset 2 (Table S2) was randomly generated from dataset 1 to deal with unbalanced sequences. Additionally, dataset 3 (Table S3) was used to compare MPXV with other *Orthopoxviruses* for phylogenetic analysis. For this, 167 *Orthopoxviruses* sequences were downloaded from GenBank, including BPXV (n = 8), CPXV (n = 32), ECTV (n = 12), VACV (n = 28), VARV (n = 22) and MPXV (n = 65). All the sequences were aligned using MAFFT (v7.490) [23] and were manually modified in MEGA6 [24]. And dataset 1 and dataset 3 were only utilized for phylogenetic analysis.

2.2. Recombination analysis

The probability of recombination events in the MPXV sequences was examined by two different approaches. First, the Neighbor-Net method in SplitsTree4 [25] was used to analyze the aligned complete genomes of 65 MPXV isolates. Compared with typical bifurcated phylogenetic trees, SplitsTree4 revealed reticular structure in the evolutionary connections across taxa [26]. Such reticulation could indicate the occurrence of recombination and if so, then the recombinants were further confirmed by RDP4 [27]. A total of seven different methods were implemented to detect the recombination signals, including RDP [28], GENECONCV [29], Chimaera [30], MaxChi [31], BootScan [32], Siscan [33], and 3Seq [34]. To avoid false identification, only recombination results supported by at least four of the seven methods with a *p*-value cutoff of 0.05 were included.

2.3. Phylogenetic analysis

The maximum likelihood (ML) approaches were used to conduct the phylogenetic analysis of datasets 1–3. ML trees were based on complete genome sequence using the general time-reversible plus gamma (GTR + G) distribution model and 1000 replicates generated by bootstraps in RAxML (v8.2.12)

[35]. All phylogenetic trees were manipulated and annotated by an online tool iTOL (v5) [36].

2.4. Phylodynamic analysis

To estimate the time scale of MPXV evolution, a phylodynamic analysis was performed. First, the temporal signal of dataset 2 was evaluated using TempEst (v1.5.3) [37] to detect sequences with erroneous sample dates or anomalous root-to-tip distance. Then the maximum clade credibility (MCC) tree was reconstructed using BEAST (v2.6.7) [38] with Hasegawa-Kishino-Yano (HKY) [39] nucleotide substitution models on the three partitions, strict clock, and coalescent constant population. The MCC tree was estimated over a 6×10^7 generations of Markov Chain Carlo (MCMC) chain and sampled every 1200 steps. In addition, we used a coalescent-based Bayesian skyline model to topologies the effective sampling size (ESS) over 1×10^7 reshufflings. Mixing and convergence were visually inspected using Tracer (v1.7.2) [40] after discharging the first 10% burn-in generations and all parameters' ESSs were higher than 200. The final MCC tree with divergence dates was summarized using the TreeAnnotator and illustrated using FigTree (v1.4.4).

2.5. Genetic differentiation among different MPXV demographics

According to the geographical division, we defined 7 demographics of MPXV (Table S2), distributed in Central Africa (CA), West Africa (WA), Europe (EU), Asia (AS), Australia (AUS), North America (NAm), and South America (SAm). We compared the pairwise F_{ST} (Fixation index) to measure the genetic variation among demographics and to estimate the gene flow level [41]. Hartl and Clark [42] specified F_{ST} values as follows: little differentiation (<0.05), moderate differentiation (0.05–0.15), great differentiation (0.15–0.25) and very great differentiation (>0.25), with the higher degree of genetic differentiation corresponding to a lower gene flow level.

2.6. Geographical correlation and discrete phylogeographic analysis

Bayesian Tip-Significance testing (BaTS) [43] was performed to illustrate the potential geographic effects on MPXV diversification. Three statistics of phylogeny-trait association were obtained using the MCC trees described in section 2.4. The association index (AI), parsimony score (PS), and maximum monophyletic clade (MC) with p values ≤ 0.05 were considered significant.

To investigate the geographic transmission patterns of MPXV, we specified a gamma distribution with four rate categories and executed 12 million iterations in BEAST (v2.6.7). Bayes factor (BF) tests were conducted by Bayesian stochastic search variable selection (BSSVS) [44] to build statistical support for phylogeographic diffusion process using spreaD3 (v0.9.6; BF cutoff = 3) [45]. Routes with high BF values were assumed to have a higher possibility for viral strain transmission.

2.7. Selection pressure and protein function analysis

The presence of positive amino acid sites under diversifying selection was assessed using dN-dS-based algorithms in DATAMONKEY [46]. Termination codons in alignments were previously stripped out using HyPhy (v2.2.4) [47]. Then four algorithms, Fast Unconstrained Bayesian Approximation (FUBAR), Mixed Effects Model of Evolution (MEME), Fixed Effects Likelihood (FEL), and Single Likelihood Ancestor Counting (SLAC) were used to test the achieved alignments for inferring selection [48–50]. The significance level was set to p-value <0.1 for MEME, FEL and SLAC, and the posterior probability of FUBAR was higher than 0.9. Sites were considered as positive selection when highlighted by at least three methods. For the location visualization of positive selection site, protein structure was created and rendered with PyMol [51].

2.8. Amino acid differences among *orthopoxviruses* IFNα/βBPs and sites binding probability

We Utilized Genedoc [52] to compare the IFNα/βBPs sequences of *orthopoxviruses* such as MPXV (NP_536604 and YP_010377172), CPXV (NP_619993), VACV (YP_233082), VARV (NP_042232), CMLV (NP_570591) and ECTV (NP_671685). The protein structural models were generated using AlphaFold2 [53] and then aligned in PyMol. The probability of protein binding sites was predicted by an interpretable deep learning model [54] and the outcomes were depicted with ChimeraX(v1.4) [55].

3. Results

3.1. Datasets, recombination, and phylogenetic inference

A total of 567 MPXV complete genome sequences were included in dataset 1, 64 in dataset 2, and 167 *Orthopoxviruses* genome sequences in dataset 3 (Tables S1–3). We used dataset 2 for recombination analysis using SplitsTree and Recombination Detection Program 4 (RDP4). A phylogenetic network with reticulation was constructed (Fig. 1A). The network revealed contradictory phylogenetic signals that might be ascribed to viral genome recombination. Dataset 2 was then evaluated for recombination events with the RDP4. Only one putative recombination event occurred in the KJ642614 sequence. Considering that recombination events could affect

the shape of a phylogenetic tree and lead to a loss of molecular loss [56], we eliminated the KJ642614 sequence from the subsequent phylogenetic, phylogeographic, and selection pressure analyses. The phylogeny based on dataset 1 revealed two major lineages, named clade I (Central African) and clade II (West African) (Fig. 1B), as described previously [57,58]. Based on the ML tree topology, we further divided the West African lineages into clade IIa.1 (endemic in the West African region in 2017–2018), clade IIa.2 (West African region and sporadically spread to the USA, Singapore, and the UK in 2017–2021), and clade IIb (2022 current outbreak). We found that two sequences collected in May 2022 in Florida and Virginia (ON674051, ON675438) were strikingly similar to the sequence from the July 2021 outbreak in Texas (ON676708), belonging to the same IIa.2 subclade. This finding coincides with other reports [59,60], implying the possibility of local transmission of MPXV within the USA before the current MPXV outbreak. Further, the cases of the clade IIb have been predominantly reported in the region of Americas and European region [7,61]. The ML tree constructed from dataset 2 (Fig. 1C) resembles the findings of dataset 1, demonstrating the confidence of the sequences we randomly chose. In addition, we explored the relationship among *orthopoxviruses* in terms of evolution using dataset 3 (Fig. 1D), where the ECTV, CPXV and VARV belong to the same clade, and BPXV, VACV, and MPXV belong to another large subclade. In conclusion, among the analyzed *orthopoxviruses*, MPXV is more similar to VACV, indicating a potential common ancestor.

3.2. Evolutionary dynamics of MPXV

The root-to-tip divergence against the sampling date in TempEst (Fig. 2A, $R^2 = 0.91$), revealed that the MPXV sampling date in dataset 2 was adequate to correct the molecular clock in the subsequent time-calibrated analysis. According to the Bayesian phylodynamic analysis, the results of the clustering are presented in the format of MCC tree (Fig. 2B) and were highly consistent with those of the phylogenetic analysis (Fig. 1C). Based on the MCC tree, we estimated the tMRCA of MPXV to be year 1969.93 (95% HPD: 1969.79–1970.00). The tMRCA of the clade II was 2000.01 (95% HPD:

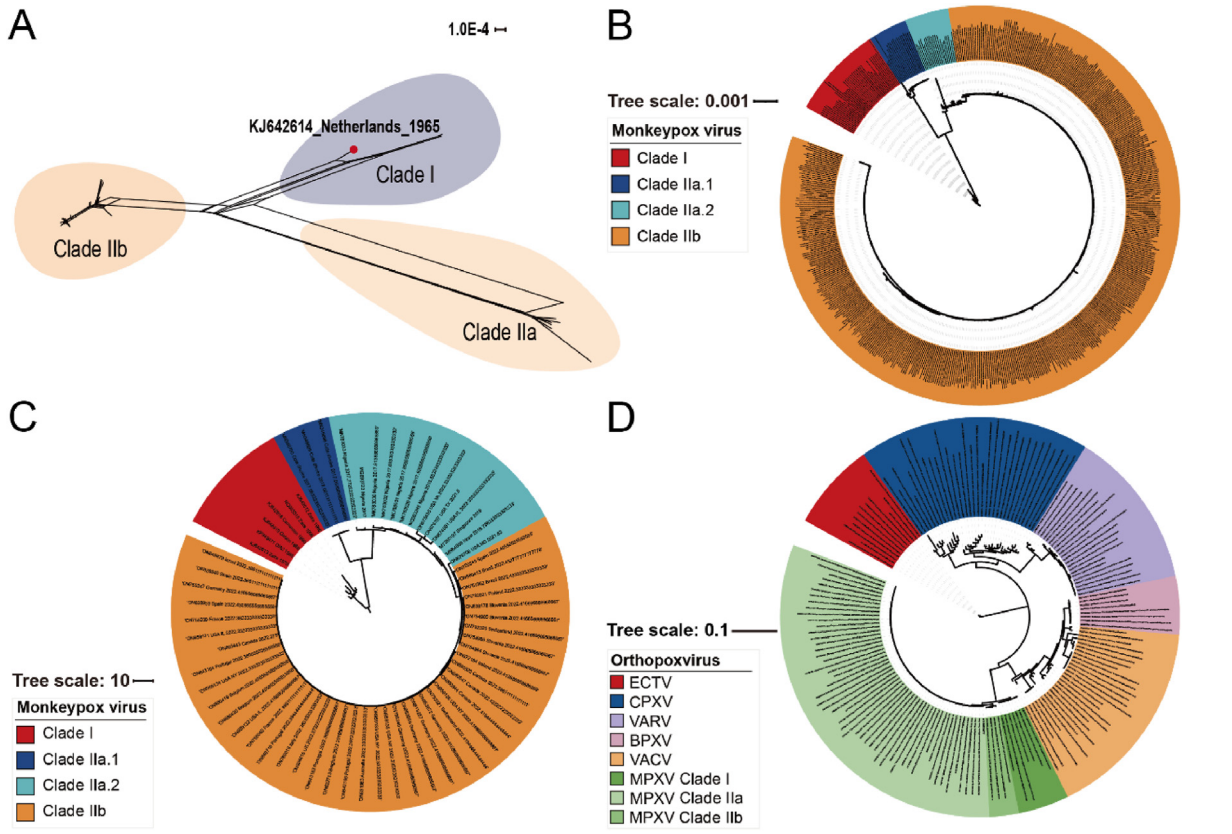

FIG. 1. Phylogenetic analysis of MPXV. (A) Phylogenetic network of MPXV's complete genome from dataset 2. The red dot represents a probable recombination event. (B) Maximum likelihood (ML) phylogenetic tree constructed with all MPXV sequences based on dataset 1. (C) ML tree of MPXV based on dataset 2. (D) ML tree of *orthopoxviruses* based on dataset 3. (For interpretation of the references to colour in this figure legend, the reader is referred to the Web version of this article.)

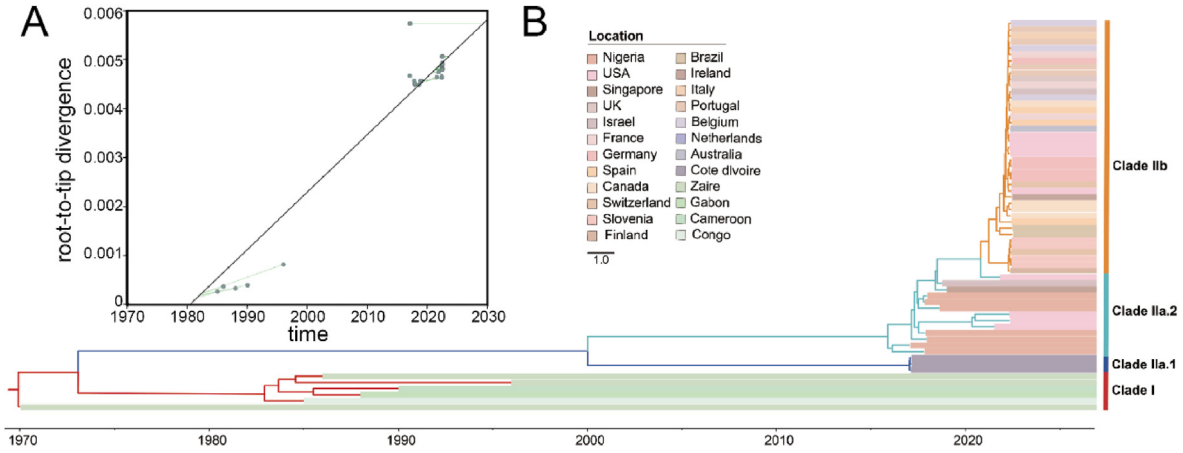

FIG. 2. Phylodynamic analysis of MPXV. (A) Linear regression between patristic and geographic distances between sampling locations in the discrete phylogeographic inference. Patristic distances were computed on the MCC tree obtained from the phylogeographic analysis performed with the BSSVS. (B) Maximum clade credibility (MCC) tree of MPXV from different countries. Strains in red regions correspond to the Clade I, ones in dark blue and sea green correspond to the early WA lineage, Clade IIa, and others in orange represent regions of the current outbreak Clade IIb. (For interpretation of the references to colour in this figure legend, the reader is referred to the Web version of this article.)

1998.85–2001.23), with 2017.02 (95% HPD: 2016.97–2017.06) for the clade IIa.1, 2015.89 (95% HPD: 2015.55–2016.24) for the clade IIa.2, and 2021.25 (95% HPD: 2020.47–2021.12) for the clade IIb. Additionally, the molecular clock estimates for dataset 2 were 7.75×10^{-5} (95% HPD: $7.35\times10^{-5} - 8.18\times10^{-5}$) substitutions/site/year. The Bayesian skyline plot depicts the relative genetic diversity of MPXV worldwide, where its population size remained constant until 2015, followed by a sharp decline between 2015 and 2017, stabilizing at a lower level, and is presently showing a moderate decrease. This demonstrates a diminution in the relative genetic diversity of MPXV.

3.3. Genetic differentiation and phylogeographic analysis

To explicate the global migration and demographic history of MPXV, we grouped the sequences into seven distinct geographic categories: CA, WA, EU, AS, AUS, NAm, and SAm. Nevertheless, the pairwise F_{ST} value was calculated among 6 populations (only one viral sequence belongs to AUS). We discovered 6 pairwise regions with F_{ST} value >0.25 (Fig. 3A), indicating that there is a significant spatial genetic divergence between MPXV from WA and those from other regions (except CA). Then we performed BaTS analysis to confirm the structure of the evolutionary diffusion of MPXV, and surprisingly found that MPXV has a considerable phylogeny-trait association in CA, WA, EU, and NAm ($p \leq 0.05$) (Table 1), indicating that the gene flow across MPXV sequences detected in these regions is limited.

A phylogeographic analysis was performed to gain further insight into the worldwide transmission patterns of MPXV. The spatial distribution of MPXV showed that there are six migration pathways: with two originating from NAm to EU (BF>10000) and AS ($BF = 24.11$), two from CA to NAm ($BF = 4.72$) and AUS ($BF = 22.16$), one from WA to NAm ($BF = 4.01$) and one from EU to AUS ($BF = 4.65$). (Fig. 3B; Table S6).

3.4. Protein structure analysis of the sites under selection pressure

We identified two codons under positive selection, residues 130 in E13L-encoded protein (Rifampicin resistance protein) and 102 in B6R-encoded protein (EEV type-I membrane glycoprotein), respectively (Table 2). Since no post-fusion structure of MPXV E13L-encoded protein is available, we used the structure of D13L-encoded protein from VACV (PDB file 2YGC) to display the amino acid location, which has 98.91% amino acid similarity with MPXV E13L-encoded protein. In addition, we predicted the protein structure of E13L-encode protein, which is highly similar to that of D13L-encoded protein, as shown in Fig. S1. D13L-encoded protein consists of two jellyrolls (J1 and J2) and a head domain of novel fold arranged as trimers (Fig. 4A) [62]. The D13L-encoded protein is a scaffold for spherical immature viral particle morphogenesis and is a specific target of rifampicin [63,64]. The amino acid site 130 is in the J1 domain near the H3 helix, on the inner side of the ring in the trimer (Fig. 4B). In the B6R-encoded protein, the positively selected amino acid, Asn 102, is in the short consensus

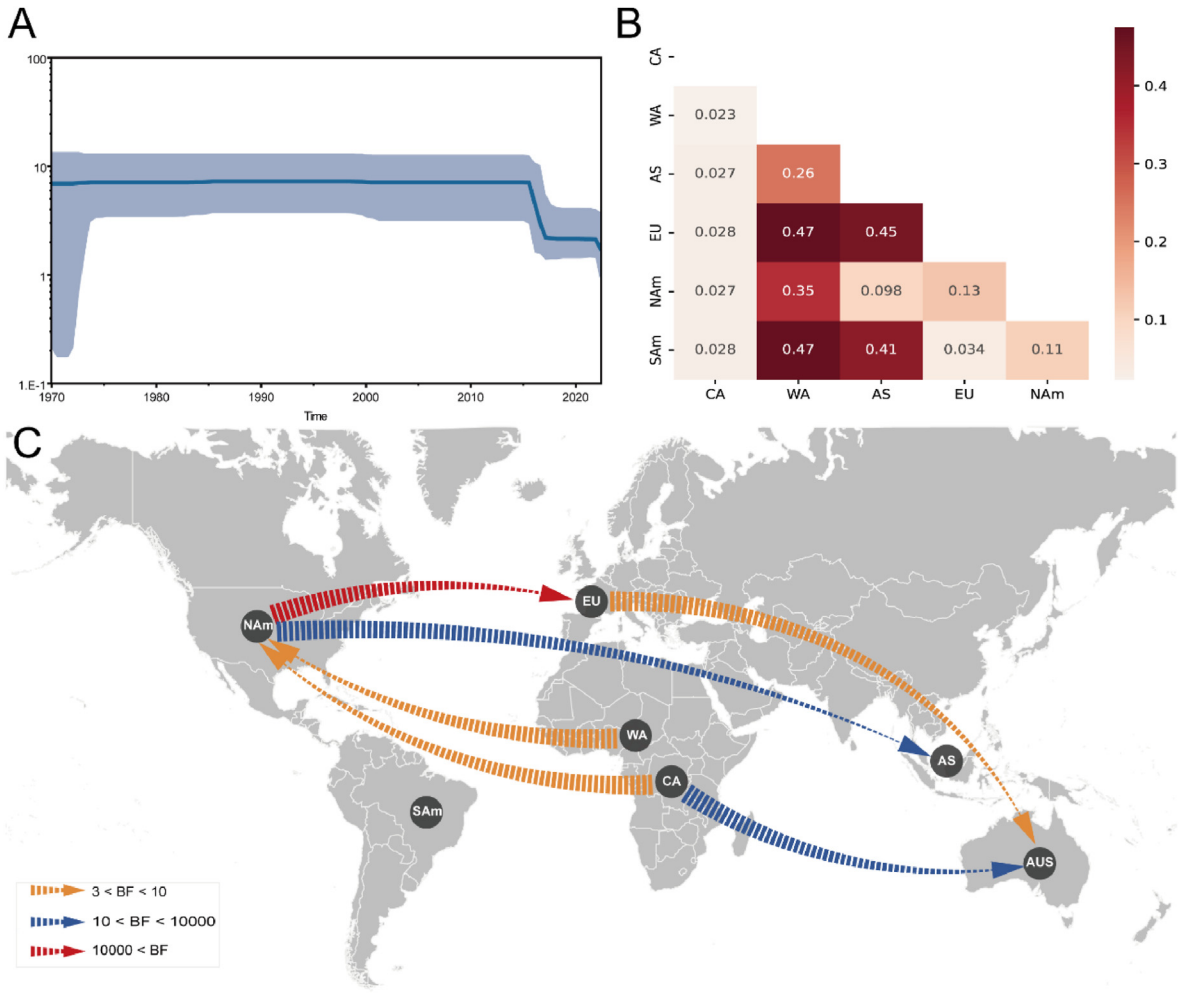

FIG. 3. Spatial diffusion of MPXV. (A) Demographic history is shown by a Bayesian skyline plot. The light blue shading represents 95% HPD of the effective population size $N_e(t)$ while the blue line is the mean value. (B) Pairwise F_{ST} of MPXV populations from genetic variation analysis. (C) Spatial diffusion pathway of MPXV using Bayesian stochastic search variable selection (BSSVS) approach. (For interpretation of the references to colour in this figure legend, the reader is referred to the Web version of this article.)

repeat (SCR) 2 domain (Fig. 4C). VACV B5R-encoded protein is a homologous protein of B6R-encoded protein (98.11% similarity) with a large extracellular domain comprised of four short consensus repeat (SCR) structural domains followed by a stalk [65]. B5R-encoded protein is the most common target of host-neutralizing antibodies among the five EEV outer membrane surface antigens of the VACV, and its expression is essential for viral morphogenesis and EEV production [66–68].

TABLE 1. Results of Bayesian Tip-association Significance testing (BaTS) for the geographical on the genetic diversity of MPXV.

Statistic	Observed mean	Lower 95% CI	Upper 95% CI	Null mean	Lower 95% CI	Upper 95% CI	Significance
AI	1.209	0.659	1.784	4.865	4.186	5.411	0.000
PS	15.126	14.000	16.000	32.500	30.474	34.321	0.000
MC (CA)	4.992	5.000	5.000	1.152	1.000	1.924	0.010
MC (WA)	3.029	3.000	3.000	1.449	1.042	2.013	0.010
MC (AS)	1.002	1.000	1.000	1.034	1.000	1.042	1.000
MC (EU)	6.240	6.000	7.000	2.724	2.132	3.993	0.010
MC (AUS)	1.000	N/A	N/A	N/A	N/A	N/A	N/A
MC (NAm)	3.079	3.000	3.000	1.764	1.177	2.998	0.040
MC (SAm)	1.444	1.000	2.000	1.007	1.000	1.020	1.000

TABLE 2. Positively selected codon sites of MPXV.

Site	FEL (p-value)	SLAC (p-value)	MEME (p-value)	FUBAR (Post.Pro)
39933	0.173	0.514	0.03	0.948
32271	0.115	0.399	0.05	0.952
107263	0.069	0.389	0.08	0.951
107558	0.138	0.217	0.09	0.945
165426	0.057	0.141	0.03	0.965
165424	0.426	0.520	0	0.911
164165	0.135	0.370	0.03	0.951
167055	118.768	0.753	0.03	0.93
170474	0.118	0.448	0.04	0.951
171695	0.212	0.446	0.05	0.94
168597	0.301	0.450	0.08	0.933
167288	0.366	0.581	0.09	0.931

3.5. Comparison of different *orthopoxviruses* IFNα/βBPs

Herein, we aimed to explore whether the amino acids of the IFNα/βBPs of MPXV varied from those of other *orthopoxviruses*, leading to differences in virus virulence and binding capacity. Multiple sequence alignment revealed that IFNα/βBPs in *orthopoxviruses* are relatively conserved. There are only two amino acid variations between MPXV clade I and clade II, where the MPXV clade II has an aspartate residue at location 178 instead of lysine in the case of MPXV clade I (Fig. S2). We subsequently focused on VACV and MPXV and found that their IFNα/βBPs differ in fifteen amino acids out of 351 amino acids (4.3% of the complete protein sequence). Fig. 5A and B depict the locations of the different amino acid (labeled as dark orange sticks). In MPXV IFNα/βBP, residues 2, 8, 15 and 52 are positioned in the N-terminal signal peptides, Trp148 and Ser151 are in the bottom loop between the two Ig-like domains, substituted Arg and Pro respectively. And the remaining nine amino acids are all located in the helix of the Ig-like domains (II and III). When integrated with the IFNα/βBP binding sites results predicted by a deep learning network, amino acids different from those corresponding to the VACV position, Trp148, Tyr163, and Leu298, situated on the IFNα/βBP and interferon binding surface, exhibited a higher binding probability (Fig. 5C). Interestingly, in the proposed protein binding model, N-terminal signal peptides show high binding potential, providing considerable

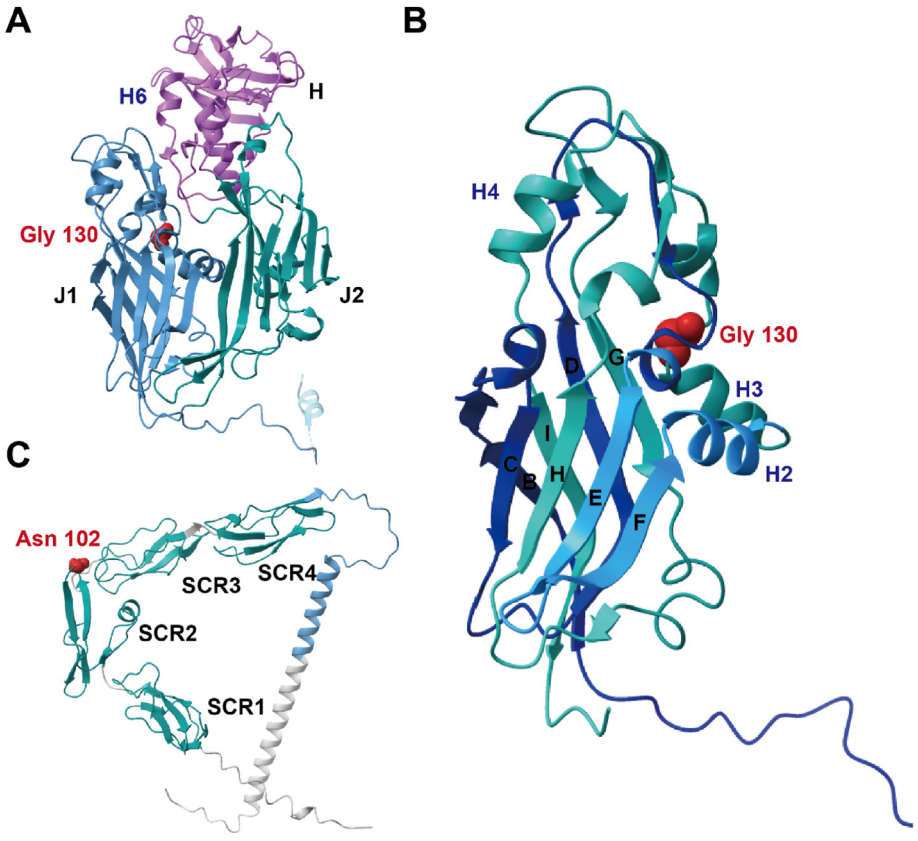

FIG. 4. Locations of adaptive amino acids in the structure of protein. (A) Structure of VACV D13L-encoded protein (PDB: 2ygc) A chain, with J1 and J2 domains in steel blue and teal respectively, and the head domain in pink. Selected amino acids are shown as red spheres. (B) Structure of VACV D13L-encoded protein J1 domain. Selected amino acids are shown as red spheres. (C) Structure predicted by Alphafold2 for the MPXV B5R-encoded protein, including four SCR-like domains in teal and a stalk in steel blue. Adaptive amino acids are represented as red spheres. (For interpretation of the references to colour in this figure legend, the reader is referred to the Web version of this article.)

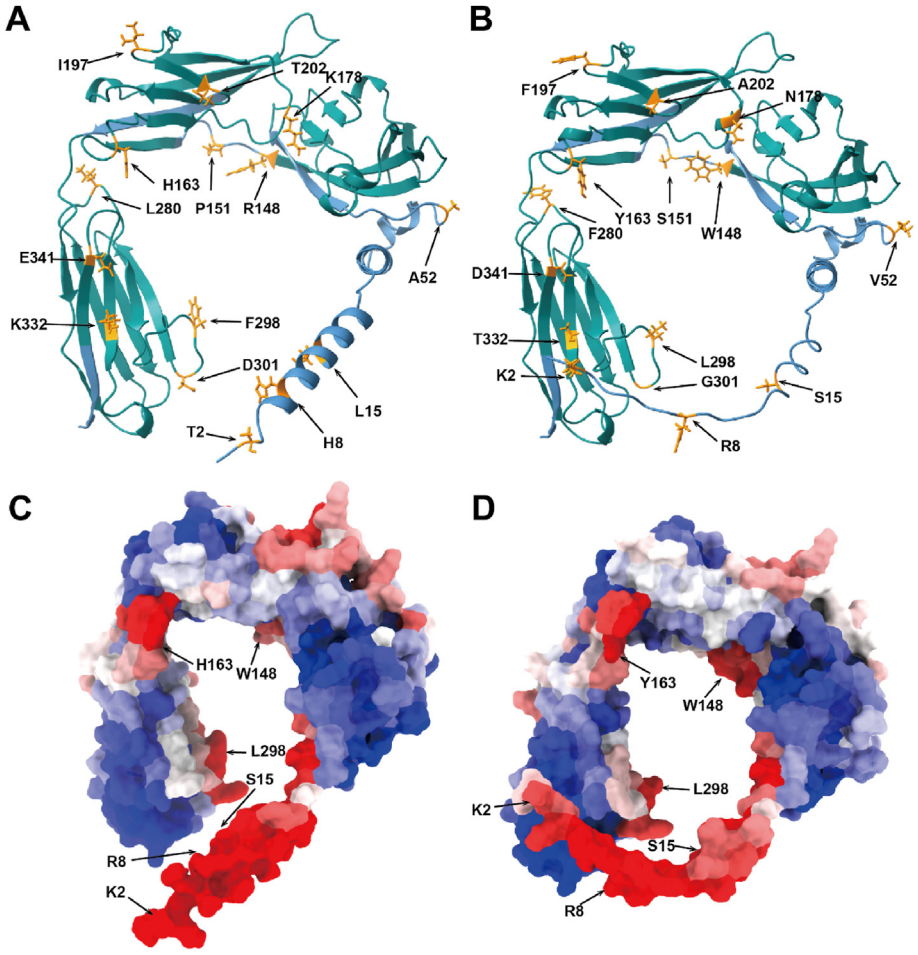

FIG. 5. Different amino acids and binding capacity prediction of IFNα/βBP. (A- and B) Structure predicted by Alphafold2 for the VACV B18R-encode protein and MPXV B16R-encoded protein respectively, the Ig-like domains displayed in teal and the N-terminal signal peptide is decorated in steel blue. The variation amnio acids are represented as orange sticks (Alphafold2 prediction results in supplementary material). (C- and D) Protein binding sites of the VACV B18R-encoded protein and MPXV B16R-encoded protein predicted by deep learning network (results in supplementary material). Red denotes a high binding probability, whereas the blue indicates a low binding probability. (For interpretation of the references to colour in this figure legend, the reader is referred to the Web version of this article.)

support for previous studies demonstrating that B18R proteins may attach to the surface of infected cells through N-terminal signaling sequences (Fig. 5C and D). Further analysis revealed that the altered amino acids 2, 8, and 15 reflected a lower binding propensity at MPXV, suggesting that the MPXV IFNα/βBP may possess a reduced capability to attach to the cell surface (Table 3).

TABLE 3. Protein binding ability of various amino acids in the VACV and MPXV interferon receptor proteins.

Residue Index	MPXV Sequence	Binding site probability	VACV Sequence	Binding site probability
2	K	**0.597**	T	**0.721**
8	R	**0.78**	H	**0.795**
15	S	**0.685**	L	**0.894**
52	V	0.2	A	0.065
148	W	**0.669**	R	**0.538**
151	S	0.419	P	0.481
163	Y	**0.69**	H	**0.676**
178	N	0.123	K	0.198
197	F	0.394	I	0.206
202	A	0.344	T	0.421
280	F	0.383	L	0.308
298	L	**0.652**	F	**0.719**
301	G	0.115	D	0.23
332	T	0.079	K	0.073
341	D	0.202	E	0.193

4. Discussion

The outbreak of MPXV in non-endemic regions has piqued the attention of many researchers, and some publications have meritoriously sought to investigate this virus for clinical

manifestations, epidemiology, and vaccines [61,69–71]. Nevertheless, current studies of the evolutionary dynamics and spatial diffusion remain to be insufficient due to the use of sparse data and basic analysis approaches [72–74]. Point to these phenomena, this study aimed at thoroughly comprehending the evolutionary history and phylogeographic transmission of MPXV by integrating a variety of bioinformatics methods based on an updated sequencing dataset spanning more than 50 years.

Despite several efforts, existing datasets are still uneven and potentially biased due to the absence of annotation information from earlier sequence data and the current intensive submission of viral sequences. The limited genetic diversity and the high similarity of recent sequences can lead to an underestimation bias in the overall time scale [75]. Therefore, particular care was devoted to balancing the temporal distribution of the data and randomly generating dataset 2 with different geographical features. The origin of MPXV was traced back to 1969.93 (95% HPD:1969.79–1970.00) for dataset 2 considered separately, which is consistent with the finding of other study [22]. However, compared to the time MPXV was first identified in 1958, our putative tMRCA is 10 years later [3], perhaps as a consequence of the scarcity of historical data and long branches hindering the accuracy of inferences on the geographical history of older viral strains [76]. The emergence of clade IIb responsible for the current outbreaks have been estimated to have originated as early as 2021.25 (95% HPD:2020.47–2021.12), implying an earlier ancestor for the 2022 MPXV than that estimates by Nextstrain (2022.01). Furthermore, based on more extensive spatiotemporal acquisition data and the branching of ON676708 in the MCC tree, we propose a distinct hypothesis from Luna [22] that the ongoing outbreak may have been spreading secretly for at least a year before it was detected in Europe. Consequently, we estimated the evolutionary rate of the MPXV complete gene averaged 7.75×10^{-5} substitutions/site/year. The mutation accumulation rate for other *orthopoxviruses* has been reported to be approximately 1.7×10^{-6}–1×10^{-5} substitutions/site/year [77–80]. The complete genome dataset reveals several traits that may have additional contributions to mutation rate estimations, while previous studies mainly centered on hemagglutinin sequences [81]. However, compared to RNA viruses like SARS-CoV-2, which evolves at a rate of 1.19×10^{-3} -6.58×10^{-3} substitutions/site/year [82,83], the mutation rate of poxviruses is relatively lower. Because they perform high fidelity DNA replication via a viral DNA polymerase with a 3'-5' exonuclease proofreading activity [84].

Our study shows the global discrete phylogeographic analysis of MPXV. Based on BaTS analysis, we obtained a compelling association between MPXV and geography, except for SAm, AS, and AUS due to the inadequacy of sequences from these regions. Our results imply that when the MPXV distributes to different regions, it will have a strong evolutionary potential to adapt to the local ecology, which is consistent with our phylogenetic findings. Furthermore, the geographical reconstruction incorporates a directional tendency through the BSSVS methods, suggesting that the linkages with the Asian countries were more likely to be facilitated through viral strains transmission with NAm rather than other African countries. Although this may seem counterintuitive at first glance, we should emphasize that for Europe, where MPXV cases are currently the most reported in the world, we merely estimated plausible transmission pathways from North America into Europe. In summary, the spatial diffusion model portrays that Africa acted as the primary seeding population while NAm established epidemiological linkers with other continents in this intricacy spread network. Apart from these results, it is critical to emphasize that under the SARS-CoV-2 pandemic, international travel has not yet completely resumed, and many countries have implemented a series of measures, so the transmission potential of the MPXV may have been underestimated due to anthropogenic constraints.

Selection pressure analysis identified two positive codons, localized in the E13L scaffold protein and EEV membrane glycoprotein. Differing from other enveloped viruses, the membrane of MPXV is generated by assembling a cytoplasmic membrane precursor onto a viral protein scaffold expressed by the E13L gene, resulting in immature viral (IV) particles [85]. The positive selection site of Gly130 is neither present in the previously random mutagenized D13 mutant library nor located in the F-loop where protein interacts with rifampin [86,87], suggesting that there may have potential mutations in E13L of MPXV that distinguish from VACV but could not react appreciably to rifampin inhibition. Likewise, the specific function of the positively selected site of Asn102 in the EEV membrane glycoprotein is hard to speculate. Although further confirmation is required, this scenario might be ascribed to the MPXV's less natural selection induced by the host, which could be interpreted as evidence of its lower virulence, resulting in less activation of the immune response. Unfortunately, there are no valid experimental *in vitro* and/or *in vivo* models available to investigate MPXV immunopathogenesis, which is likely the most compelling and relevant evidence to corroborate its evolutionary history. However, the progressive accumulation of burgeoning mutations favors the formation of a distinct adaptive mutation [88]. As a result, the panel of mutations described here might be valuable for MPXV immunology and may elucidate the plausibility of cumulative mutation hypothesis by further confirmation.

The current therapeutic drugs and vaccines for MPXV are those used for VARV, but the virulence of different

orthopoxviruses varies. Here we performed a comparative analysis of IFNα/βBP, a specific virulence protein of orthopox virus that can act as a soluble extracellular and cell surface protein [89]. Our results show that the Ig I region of MPXV and VACV is relatively conserved. Coupled with Montanuy et al.'s [90] finding showing that the IFNα/βBP of VACV mediates interactions with cell surface glycosaminoglycans (GAGs) at the basic residue cluster of the Ig I domain, we propose that the function of MPXV IFNα/βBP and GAGs binding sites is maintained. These findings could contribute to an expansive understanding of MPXV immune regulation and facilitate the design of intervention strategies. Our deep learning networks show that the three amino acid variations in the amino terminus, which have been confirmed to be crucial for cell binding capacity in a previous work [91], resulted in a decrease in the IFNα/βBP binding ability of MPXV. IFNα/βBP is secreted by infected cells and impede IFN deliver to the target sites after binding to the cell surface in solution, suppressing the formation of an antiviral state in surrounding uninfected cells [16,89]. The diminished capacity of the amino-terminal portion of the IFNα/βBP to attach to cells, resulting in a lesser capability to inhibit IFN release, may also contribute to MPXV's weaker pathogenicity. Particularly, orthologues of the intracellular poxvirus resistance proteins E3 and K3 are intact in VARV but truncated or absent in MPXV [92], indicating that MPXV is more reliant than other poxviruses on the modulation of the host's immune response by secreted type I IFN inhibitors. IFNα/βBPs are abundantly expressed in MPXV-infected cells which have the potential to work as viral immunomodulatory proteins. They can serve as target for therapeutically virulent MPXV as well as component of MPXV protective vaccines. Subunit vaccines against MPXV comprise structural proteins expressed in VACV particles, with virulence factors secreted by the virus as complementary components that cooperate to neutralize the infectivity of MPXV [93,94]. The insertion of a full-length IFNα/βBP, or a mutant lacking IFN-binding activity in the vaccine, could induce a stronger anti-IFN response and enhance its protective effect. Furthermore, monoclonal antibodies against the MPXV IFNα/βBP protein might be effective as pharmaceutical compounds to prevent disease in exposed human MSM (men who have sex with men) or HIV (human immunodeficiency virus) patients. Hence, this would be a desirable alternative for people who are at high risk of facing serious adverse reactions owing to immunodeficiency [95].

In summary, the present study provides an updated representation of MPXV evolutionary dynamics, phylogeography and adaptation, pointing out a quite fast evolutionary rate, discovering dependable spatial diffusion and two potential adaptive amino acids compared to other studies of MPXV molecular evolution. These results support the notion that the ongoing MPXV epidemic features a cryptic molecular evolution and intricate spatiotemporal transmission patterns. It is worth mentioning that the current work just scratched the surface of MPXV evolution history and further surveillance on the epidemiology, natural adaption, and pathogenesis of MPXV is required. Additionally, the integration of pertinent epidemiological information with genetic monitoring data would assist to implement appropriate prevention and control measures, as well as optimizing public health decisions to mitigate epidemics.

Funding

This work was supported by the National Natural Science Foundation of China [grants 31970752]; the Science, Technology, Innovation Commission of Shenzhen Municipality [JCYJ20190809180003689, JSGG20200225150707332, JSGG20191129110812708, ZDSYS20200820165400003, WDZC20200820173710001, JCYJ20220530014301 4032]; and the Shenzhen Bay Laboratory Open Funding [SZBL2020090501004].

Declaration of competing interest

The authors declare that they have no known competing financial interests or personal relationships that could have appeared to influence the work reported in this paper.

CRediT authorship contribution statement

Haifei Guan: Conceptualization, Methodology, Software, Validation, Formal analysis, Writing – original draft. **Ijaz Gul:** Conceptualization, Writing – review & editing. **Chufan Xiao:** Writing – review & editing. **Shuyue Ma:** Writing – review & editing. **Yingshan Liang:** Writing – review & editing. **Dongmei Yu:** Writing – review & editing. **Ying Liu:** Writing – review & editing. **Hong Liu:** Writing – review & editing. **Can Yang Zhang:** Writing – review & editing. **Juan Li:** Writing – review & editing. **Peiwu Qin:** Conceptualization, Writing – review & editing, Funding acquisition.

Appendix A. Supplementary data

Supplementary data to this article can be found online at https://doi.org/10.1016/j.nmni.2023.101102.

References

[1] Sklenovska N, Van Ranst M. Emergence of monkeypox as the most important orthopoxvirus infection in humans. Front Public Health 2018;6:241.

[2] Yinka-Ogunleye A, Aruna O, Dalhat M, et al. Outbreak of human monkeypox in Nigeria in 2017–18: a clinical and epidemiological report. Lancet Infect Dis 2019;19:872–9.

[3] Cho CT, Wenner HA. Monkeypox virus. Bacteriol Rev 1973;37:1–18.

[4] Breman JG, Steniowski M, Zanotto E, et al. Human monkeypox, 1970-79. Bull World Health Organ 1980;58:165.

[5] Seang S, Burrel S, Todesco E, et al. Evidence of human-to-dog transmission of monkeypox virus. Lancet 2022;400:658–9.

[6] WHO. Monkeypox outbreak: global trends. Available online:https://worldhealthorg.shinyapps.io/mpx_global/, . [Accessed 12 February 2023].

[7] Organization WH. Monkeypox outbreak: global trends. https://worldhealthorg.shinyapps.io/mpx_global/; 2022.

[8] Fenner F, Henderson DA, Arita I, et al. Smallpox and its eradication. World Health Organization Geneva; 1988.

[9] Earl PL, Americo JL, Wyatt LS, et al. Rapid protection in a monkeypox model by a single injection of a replication-deficient vaccinia virus. Proc Natl Acad Sci USA 2008;105:10889–94.

[10] Li H, Zhang H, Ding K, et al. The evolving epidemiology of monkeypox virus. Cytokine Growth Factor Rev 2022;68:1–12.

[11] Randall RE, Goodbourn S. Interferons and viruses: an interplay between induction, signalling, antiviral responses and virus countermeasures. J Gen Virol 2008;89:1–47.

[12] Katze MG, He Y, Gale M. Viruses and interferon: a fight for supremacy. Nat Rev Immunol 2002;2:675–87.

[13] Chang HW, Watson JC, Jacobs BL. The E3L gene of vaccinia virus encodes an inhibitor of the interferon-induced, double-stranded RNA-dependent protein kinase,. Proc Natl Acad Sci USA 1992;89:4825–9.

[14] Beattie E, Tartaglia J, Paoletti E. Vaccinia virus-encoded eIF-2α homolog abrogates the antiviral effect of interferon. Virology 1991;183:419–22.

[15] Bratke KA, McLysaght A, Rothenburg S. A survey of host range genes in poxvirus genomes, Infection,. Genetics and Evolution 2013;14:406–25.

[16] Alcamí A, Symons JA, Smith GL. The vaccinia virus soluble alpha/beta interferon (IFN) receptor binds to the cell surface and protects cells from the antiviral effects of IFN,. J Virol 2000;74:11230–9.

[17] Fernández de Marco MdM, Alejo A, Hudson P, et al. The highly virulent variola and monkeypox viruses express secreted inhibitors of type I interferon,. Faseb J 2010;24:1479–88.

[18] Alcami A, Smith GL. A soluble receptor for interleukin-1β encoded by vaccinia virus: a novel mechanism of virus modulation of the host response to infection,. Cell 1992;71:153–67.

[19] Chakraborty C, Bhattacharya M, Sharma AR, et al. Evolution, epidemiology, geographical distribution, and mutational landscape of newly emerging monkeypox virus. GeroScience 2022:1–17.

[20] Shete AM, Yadav PD, Kumar A, et al. Genome characterization of monkeypox cases detected in India: identification of three sub clusters among A. 2 lineage. J. Infect. 2023;86:66–117.

[21] Scarpa F, Sanna D, Azzena I, et al. Genetic variability of the monkeypox virus clade IIb B. 1. J. Clin. Med. 2022;11:6388.

[22] Luna N, Ramírez AL, Muñoz M, et al. Phylogenomic analysis of the monkeypox virus (MPXV) 2022 outbreak: emergence of a novel viral lineage? Trav Med Infect Dis 2022;49:102402.

[23] Katoh K, Standley DM. MAFFT multiple sequence alignment software version 7: improvements in performance and usability. Mol Biol Evol 2013;30:772–80.

[24] Tamura K, Stecher G, Peterson D, et al. MEGA6: molecular evolutionary genetics analysis version 6.0. Mol Biol Evol 2013;30:2725–9.

[25] Huson DH. SplitsTree: analyzing and visualizing evolutionary data. Bioinformatics (Oxford, England) 1998;14:68–73.

[26] Huson DH, Bryant D. Application of phylogenetic networks in evolutionary studies. Mol Biol Evol 2006;23:254–67.

[27] Martin DP, Murrell B, Golden M, et al. RDP4: detection and analysis of recombination patterns in virus genomes. Virus evolution 2015:1.

[28] Martin D, Rybicki ERDP. Detection of recombination amongst aligned sequences. Bioinformatics 2000;16:562–3.

[29] Padidam M, Sawyer S, Fauquet CM. Possible emergence of new geminiviruses by frequent recombination. Virology 1999;265:218–25.

[30] Posada D, Crandall KA. Evaluation of methods for detecting recombination from DNA sequences: computer simulations. Proc Natl Acad Sci USA 2001;98:13757–62.

[31] Smith JM. Analyzing the mosaic structure of genes. J Mol Evol 1992;34:126–9.

[32] Martin D, Posada D, Crandall K, et al. A modified bootscan algorithm for automated identification of recombinant sequences and recombination breakpoints. J Virol 2005:95.

[33] Gibbs MJ, Armstrong JS, Gibbs AJ. Sister-scanning: a Monte Carlo procedure for assessing signals in recombinant sequences. Bioinformatics 2000;16:573–82.

[34] Boni MF, Posada D, Feldman MW. An exact nonparametric method for inferring mosaic structure in sequence triplets. Genetics 2007;176:1035–47.

[35] Stamatakis A. RAxML version 8: a tool for phylogenetic analysis and post-analysis of large phylogenies. Bioinformatics 2014;30:1312–3.

[36] Letunic I, Bork P. Interactive Tree of Life (iTOL) v5: an online tool for phylogenetic tree display and annotation. Nucleic Acids Res 2021;49:W293–6.

[37] Rambaut A, Lam TT, Max Carvalho L, et al. Exploring the temporal structure of heterochronous sequences using TempEst (formerly Path-O-Gen). Virus evolution 2016;2. vew007.

[38] Bouckaert R, Heled J, Kühnert D, et al. BEAST 2: a software platform for Bayesian evolutionary analysis. PLoS Comput Biol 2014;10.e1003537.

[39] Hasegawa M, Kishino H. Yano T-a. Dating of the human-ape splitting by a molecular clock of mitochondrial DNA. J Mol Evol 1985;22:160–74.

[40] Rambaut A, Drummond AJ, Xie D, et al. Posterior summarization in Bayesian phylogenetics using Tracer 1.7. Syst Biol 2018;67:901–4.

[41] Neigel JE. Estimation of effective population size and migration parameters from genetic data, Molecular genetic approaches in conservation. 1996. p. 329–46.

[42] Hartl DL, Clark AG, Clark AG. Principles of population genetics. Sinauer associates Sunderland 1997.

[43] Parker J, Rambaut A, Pybus OG. Correlating viral phenotypes with phylogeny: accounting for phylogenetic uncertainty, Infection. Genetics and Evolution 2008;8:239–46.

[44] Lemey P, Rambaut A, Drummond AJ, et al. Bayesian phylogeography finds its roots. PLoS Comput Biol 2009;5. e1000520.

[45] Bielejec F, Rambaut A, Suchard MA, et al. SPREAD: spatial phylogenetic reconstruction of evolutionary dynamics. Bioinformatics 2011;27:2910–2.

[46] Pond SLK, Frost SD. Datamonkey: rapid detection of selective pressure on individual sites of codon alignments. Bioinformatics 2005;21:2531–3.

[47] Pond SLK, Muse SV. HyPhy: hypothesis testing using phylogenies. Statistical methods in molecular evolution. Springer; 2005. p. 125–81.

[48] Murrell B, Moola S, Mabona A, et al. FUBAR: a fast, unconstrained bayesian approximation for inferring selection. Mol Biol Evol 2013;30:1196–205.

[49] Murrell B, Wertheim JO, Moola S, et al. Detecting individual sites subject to episodic diversifying selection. PLoS Genet 2012;8.e1002764.

[50] Kosakovsky Pond SL, Frost SD. Not so different after all: a comparison of methods for detecting amino acid sites under selection. Mol Biol Evol 2005;22:1208–22.
[51] Schrodinger LLC. The PyMOL molecular graphics system, Version 1.8. 2015.
[52] Nicholas KB. Genedoc: a tool for editing and annoting multiple sequence alignments. http://wwwpscedu/biomed/genedoc; 1997.
[53] Mirdita M, Schütze K, Moriwaki Y, et al. ColabFold: making protein folding accessible to all. Nat Methods 2022:1–4.
[54] Tubiana J, Schneidman-Duhovny D, Wolfson HJ. ScanNet: an interpretable geometric deep learning model for structure-based protein binding site prediction. Nat Methods 2022:1–10.
[55] Pettersen EF, Goddard TD, Huang CC, et al. UCSF ChimeraX: structure visualization for researchers, educators, and developers. Protein Sci 2021;30:70–82.
[56] Schierup MH, Hein J. Consequences of recombination on traditional phylogenetic analysis. Genetics 2000;156:879–91.
[57] Chen N, Li G, Liszewski MK, et al. Virulence differences between monkeypox virus isolates from West Africa and the Congo basin. Virology 2005;340:46–63.
[58] Organization WH. Monkeypox: experts give virus variants new names (22 October 2022, date last accessed), https://www.who.int/news/item/12-08-2022-monkeypox-experts-give-virus-variants-new-names.
[59] Isidro J, Borges V, Pinto M, et al. Phylogenomic characterization and signs of microevolution in the 2022 multi-country outbreak of monkeypox virus. Nat. Med. 2022;28:1569–72.
[60] Yadav PD, Reghukumar A, Sahay RR, et al. First two cases of Monkeypox virus infection in travellers returned from UAE to India. J. Infect. 2022;85:e145–8.
[61] Lum F-M, Torres-Ruesta A, Tay MZ, et al. Monkeypox: disease epidemiology, host immunity and clinical interventions. Nat Rev Immunol 2022;22:597–613.
[62] Bahar MW, Graham SC, Stuart DI, et al. Insights into the evolution of a complex virus from the crystal structure of vaccinia virus D13. Structure 2011;19:1011–20.
[63] Moss B, Rosenblum EN, Katz E, et al. Rifampicin: a specific inhibitor of vaccinia virus assembly. Nature 1969;224:1280–4.
[64] Sodeik B, Griffiths G, Ericsson M, et al. Assembly of vaccinia virus: effects of rifampin on the intracellular distribution of viral protein p65. J Virol 1994;68:1103–14.
[65] Engelstad M, Howard ST, Smith GL. A constitutively expressed vaccinia gene encodes a 42-kDa glycoprotein related to complement control factors that forms part of the extracellular virus envelope,. Virology 1992;188:801–10.
[66] Bell E, Shamim M, Whitbeck JC, et al. Antibodies against the extracellular enveloped virus B5R protein are mainly responsible for the EEV neutralizing capacity of vaccinia immune globulin. Virology 2004;325:425–31.
[67] Pütz MM, Midgley CM, Law M, et al. Quantification of antibody responses against multiple antigens of the two infectious forms of Vaccinia virus provides a benchmark for smallpox vaccination. Nat. Med. 2006;12:1310–5.
[68] Wolffe EJ, Isaacs S, Moss B. Deletion of the vaccinia virus B5R gene encoding a 42-kilodalton membrane glycoprotein inhibits extracellular virus envelope formation and dissemination. J Virol 1993;67:4732–41.
[69] Patel A, Bilinska J, Tam JC, et al. Clinical features and novel presentations of human monkeypox in a central London centre during the 2022 outbreak: descriptive case series. bmj 2022:378.
[70] Keasey S, Pugh C, Tikhonov A, et al. Proteomic basis of the antibody response to monkeypox virus infection examined in cynomolgus macaques and a comparison to human smallpox vaccination. PLoS One 2010;5. e15547.
[71] Kupferschmidt K. Monkeypox vaccination plans take shape amid questions. Science 2022;376:1142–3.
[72] Berthet N, Descorps-Declère S, Besombes C, et al. Genomic history of human monkey pox infections in the Central African Republic between 2001 and 2018. Sci Rep 2021;11:1–11.
[73] Nakazawa Y, Emerson GL, Carroll DS, et al. Phylogenetic and ecologic perspectives of a monkeypox outbreak, southern Sudan. Emerg Infect Dis 2005;2013(19):237.
[74] Likos AM, Sammons SA, Olson VA, et al. A tale of two clades: monkeypox viruses,. J Gen Virol 2005;86:2661–72.
[75] Duchêne D, Duchêne S, Ho SY. Tree imbalance causes a bias in phylogenetic estimation of evolutionary timescales using heterochronous sequences. Mol. Ecol.Resour 2015;15:785–94.
[76] Nelson MI, Viboud C, Vincent AL, et al. Global migration of influenza A viruses in swine. Nat Commun 2015;6:1–11.
[77] Hughes AL, Irausquin S, Friedman R. The evolutionary biology of poxviruses, Infection,. Genetics and Evolution 2010;10:50–9.
[78] Duggan AT, Perdomo MF, Piombino-Mascali D, et al. 17th century variola virus reveals the recent history of smallpox. Curr Biol 2016;26:3407–12.
[79] Firth C, Kitchen A, Shapiro B, et al. Using time-structured data to estimate evolutionary rates of double-stranded DNA viruses. Mol Biol Evol 2010;27:2038–51.
[80] Babkin I, Shchelkunov S. Molecular evolution of poxviruses. Russ J Genet 2008;44:895–908.
[81] Franzo G, He W, Correa-Fiz F, et al. A shift in Porcine circovirus 3 (PCV-3) history paradigm: phylodynamic analyses reveal an ancient origin and prolonged undetected circulation in the worldwide swine population,. Adv Sci 2019;6:1901004.
[82] Li X, Zai J, Zhao Q, et al. Evolutionary history, potential intermediate animal host, and cross-species analyses of SARS-CoV-2. J Med Virol 2020;92:602–11.
[83] Benvenuto D, Giovanetti M, Salemi M, et al. The global spread of 2019-nCoV: a molecular evolutionary analysis,. Pathog Glob Health 2020;114:64–7.
[84] Moss B. Poxvirus DNA replication. Cold Spring Harbor Perspect Biol 2013;5. a010199.
[85] Maruri-Avidal L, Weisberg AS, Moss B. Direct formation of vaccinia virus membranes from the endoplasmic reticulum in the absence of the newly characterized L2-interacting protein A30. 5. J. Virol. 2013;87:12313–26.
[86] Charity JC, Katz E, Moss B. Amino acid substitutions at multiple sites within the vaccinia virus D13 scaffold protein confer resistance to rifampicin. Virology 2007;359:227–32.
[87] Garriga D, Headey S, Accurso C, et al. Structural basis for the inhibition of poxvirus assembly by the antibiotic rifampicin. Proc Natl Acad Sci USA 2018;115:8424–9.
[88] Imai H, Dinis JM, Zhong G, et al. Diversity of influenza A (H5N1) viruses in infected humans, Northern Vietnam, 2004–2010. Emerg. Infect. Dis. 2018;24:1128.
[89] Colamonici OR, Domanski P, Sweitzer SM, et al. Vaccinia virus B18R gene encodes a type I interferon-binding protein that blocks interferon α transmembrane signaling (*). J Biol Chem 1995;270:15974–8.
[90] Montanuy I, Alejo A, Alcami A. Glycosaminoglycans mediate retention of the poxvirus type I interferon binding protein at the cell surface to locally block interferon antiviral responses. Faseb J 2011;25:1960–71.
[91] Golden JW, Hooper JW. Evaluating the orthopoxvirus type I interferon-binding molecule as a vaccine target in the vaccinia virus intranasal murine challenge model. Clin Vaccine Immunol 2010;17:1656–65.
[92] Weaver JR, Isaacs SN. Monkeypox virus and insights into its immunomodulatory proteins. Immunol Rev 2008;225:96–113.

[93] Xu R-H, Cohen M, Tang Y, et al. The orthopoxvirus type I IFN binding protein is essential for virulence and an effective target for vaccination,. J Exp Med 2008;205:981–92.

[94] Kim M, Yang H, Kim S-K, et al. Biochemical and functional analysis of smallpox growth factor (SPGF) and anti-SPGF monoclonal antibodies. J Biol Chem 2004;279:25838–48.

[95] Jacobs BL, Langland JO, Kibler KV, et al. Vaccinia virus vaccines: past, present and future. Antivir Res 2009;84:1–13.